A new active power filter topology based on a chopper circuit

Xiao-Ling Guo(郭晓玲)[1,2;1)] Jian Cheng(程健)[1;2)] Bo Zhang(张波)[3]
Jing Zhang(张旌)[1,2] Yuan Huang(黄远)[1,2]

[1] Institute of High Energy Physics, Chinese Academy of Sciences, Beijing 100049, China
[2] Dongguan Neutron Science Center, Dongguan 523803, China
[3] BoXingKeYuan Electronic Technology Co., Ltd., Beijing 101300, China

Abstract: Active power filters (APFs) are widely used for their outstanding performance in current and voltage ripple compensation. As modern high-energy accelerators are demanding much more stringent current ripple guidelines, APFs are used in the magnet power supply (MPS) in accelerator systems. However, conventional APFs have many drawbacks due to the traditional topology, such as complex structure, nonadjustable working voltage, requirement of power supply, and so on. This paper proposes a new APF topology, which works as two types of chopper circuits. This APF does not need extra electricity, but uses the power of the MPS current ripple to realize ripple depression. Experimental results prove its feasibility and effectiveness.

Keywords: active power filter, magnet power supply, current ripple compensation

PACS: 84.30.Vn, 07.50.Hp **DOI:** 10.1088/1674-1137/40/1/017005

1 Introduction

In a particle accelerator magnet power supply (MPS) system, an active power filter (APF) can effectively depress the ripples or harmonics in current and voltage, thus improving the current quality and stability in the accelerator. To compensate for the ripple component in MPS, the APF outputs a current to the magnet, which has the same amplitude but opposite phase as the MPS current ripple, thereby counteracting the current ripple through the magnet [1].

There are two types of APF, parallel-APF and series-APF. Of these, the parallel APF is used to compensate the current ripple, while the series one is used to decrease the voltage ripple. As most magnet power supplies are high-precision current sources, the parallel APF is more suitable and appropriate for accelerator MPS. Therefore, this paper only focuses on the parallel APF [2].

Obviously, in order to offset the ripple component in MPS current, the APF needs to output an AC ripple current, which means that the main circuit of APF is an inverter. Fig.1 shows a schematic for a conventional parallel APF [3].

As shown in Fig. 1, the APF mainly consists of three parts, which are the circuit, the current controller, and the current ripple detection. When the APF is working, the current ripple detection analyzes the MPS current to get the information about the ripple component, and then the APF circuit is controlled by the current controller to generate an opposite ripple current according to the detected result.

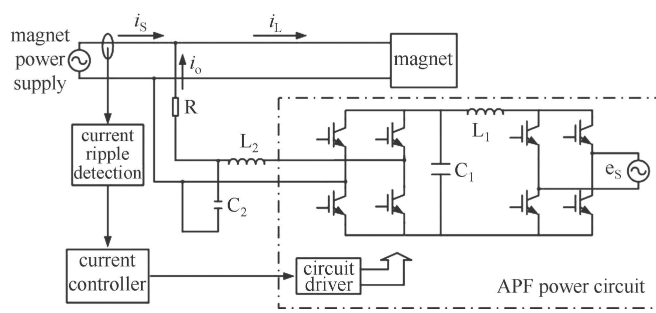

Fig. 1. Principle diagram of APF.

In Fig. 1, i_S denotes the current output by the MPS, i_o is the compensating current from the APF, and i_L is the final current through the magnet. i_S can be expressed by the following equation:

$$i_S = i_f + i_w, \tag{1}$$

where i_f represents the DC component from the MPS, and i_w is the ripple component. In order to make it contain only a DC part, the following formula should be satisfied:

$$i_o = -i_w. \tag{2}$$

Received 3 April 2015, Revised 28 August 2015

1) E-mail: guoxl@ihep.ac.cn
2) E-mail: chengj@mail.ihep.ac.cn

A conventional APF is usually composed of a rectifier and an inverter. The rectifier converts the AC to DC, and the inverter transforms the DC into ripple current, which is AC. These two devices make the structure of the APF complicated, so its volume is difficult to miniaturize, and the cost is high. In addition, as the APF is connected to the magnet in parallel with the MPS, its output voltage Vo is equal to the output voltage of the MPS, which means that a voltage balance should be made between the APF and MPS. This makes the APF difficult to apply to various MPS with different output voltages, and once the output voltage of the MPS changes, the voltage of the APF also needs to be altered.

To overcome the shortcomings described above, a new APF topology is proposed in this paper.

2 Principles of new APF topology

The principle of the new type of APF presented in this paper is shown in Fig. 2.

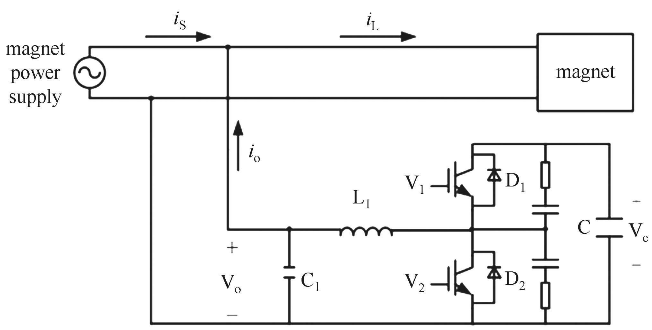

Fig. 2. Schematic of new APF topology.

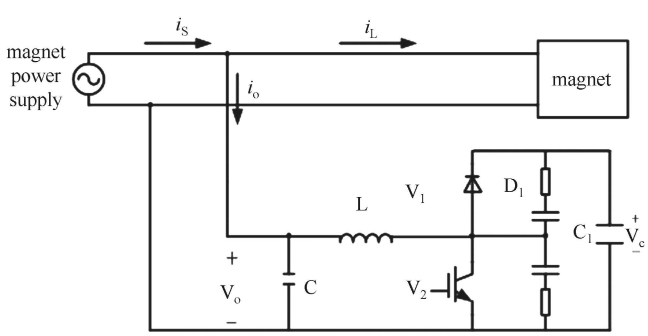

Fig. 3. APF working as a Boost circuit.

The information about the amplitude, phase and frequency of ripples can be obtained by the current ripple detection. If the detected result shows $i_w \geqslant 0$, it means there is a positive ripple current in the MPS current. At this time the APF should output a negative current, which means the APF is drawing current from the MPS. At this point, device V_2 works according to the controller while V_1 is disconnected, and the equivalent circuit diagram of this APF can be shown in Fig. 3.

As shown in Fig. 3, the APF works as a Boost converter in this operating state, and the APF circuit stores the ripple power from the MPS to the storage capacitor C_1 while V_2 is connected. In this case, the input power voltage to the AFP is the output voltage of the MPS, which is V_o, and the output voltage of this Boost circuit is the voltage across capacitor C_1, which is V_c.

The relationship between V_c and V_o can be represented as Eq. (3).

$$V_c = \frac{V_o}{1-D_2}, \tag{3}$$

where D_2 is the duty ratio of V_2.

Otherwise when $i_w < 0$, it predicates that the current ripple of the MPS is negative, so at this time the APF should output a positive ripple current, which means that the APF needs to inject a ripple current to the magnet. In this case, V_2 needs to be disconnected and V_1 works according to the controller, and then the equivalent circuit diagram can be shown in Fig. 4.

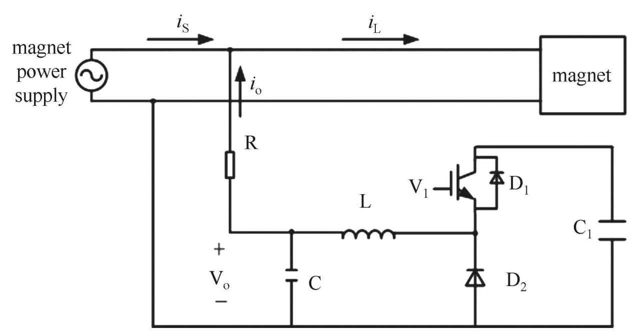

Fig. 4. APF working as a Buck circuit.

Obviously, the APF works as a Buck converter during this period. Its power source is the voltage across the capacitor C_1, and the output voltage is the MPS voltage V_o. The equation between the two voltages is expressed as Equation (4).

$$V_o = V_c \times D_1, \tag{4}$$

where D_1 is the duty ratio of device V_1.

It can be concluded from the operating process that the input and output voltages of the APF circuit are determined by the voltage of the MPS, which means it is not a fixed value, but adapts automatically to the MPS voltage. This means that the APF is very adaptive, and when the MPS outputs different voltages, the APF can catch up with the changes.

The APF can be considered as a power supply when designing its controller. However, the control loop of APF is not totally identical to that of a normal digital power supply [4]. This is because the reference of an APF circuit is not an informed value or wave as in a power supply, but the detected information about the current ripple, which is variable. Figure 5 shows the diagram of the APF control loop proposed in this paper.

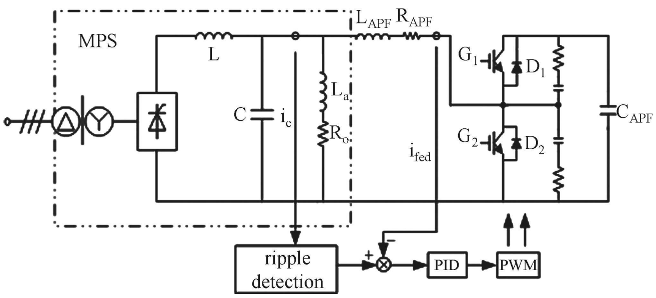

Fig. 5. Schematic of APF control loop.

3 APF prototype and experiments

In order to verify and examine the performance and effectiveness of the APF described above, an experimental system was built to test the APF, as shown in Fig. 6.

Fig. 6. (color online) Experimental APF system.

The experimental system is composed of an MPS, an APF prototype, a computer, a resistive load, and a scope. The computer is used for software debugging and parameter modulation. The main part of the MPS prototype is a three-phase full-bridge rectifier as shown in Fig. 7, which is a common topology of DC constant current power supplies. The APF in this paper is available to almost all kinds of power supply systems, and the MPS in this experiment is used to verify the effect of the APF.

The APF is produced strictly according to Fig. 2, so its working principle is shown in that figure. The controller in this APF uses a closed-loop current, and the relationship in this loop is shown in Fig. 5. In this APF controller, a field-programmable gate array (FPGA) chip is used to realize the control loop. A blocking capacitor is installed before the sampling of the MPS current, and thus the sampled signal only contains the ripple component i_w. The implementation of the control loop in the FPGA is represented in Fig. 8.

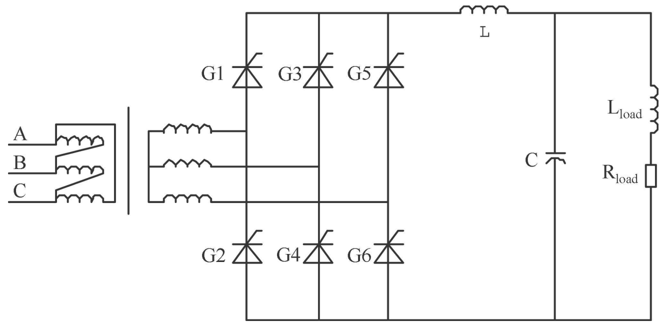

Fig. 7. Schematic of MPS prototype.

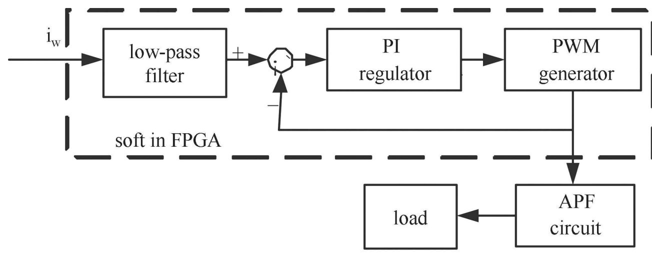

Fig. 8. APF control loop in FPGA.

In Fig. 8, the low-pass filter is used to remove the high-frequency harmonics and interference components in the sampled signal. The bandwidth of the APF is defined by this digital filter; in this paper, it is set to 1000 Hz, which is suitable for most MPS in accelerators.

As described previously, the APF is connected in parallel with the MPS to the magnet, as shown in Fig. 9.

Fig. 9. (color online) Connection of APF between power supply and load.

In order to observe the current waveform of the load directly, a resistance is used as the load, whose current waveform is the same as the voltage waveform. For the purpose of watching the changes in current ripple, the scope was set to AC observation in this experiment. Figure 10 shows the waveform of the MPS current ripple when the MPS output current was set to 24 A with the APF disconnected. As the MPS is a three-phase full-bridge rectifier, the main components of the current ripple are the frequency multiplications of 50 Hz, which comes from the grid. As can be seen from Fig. 10, the components are 50 Hz, 100 Hz, 150 Hz and 300 Hz.

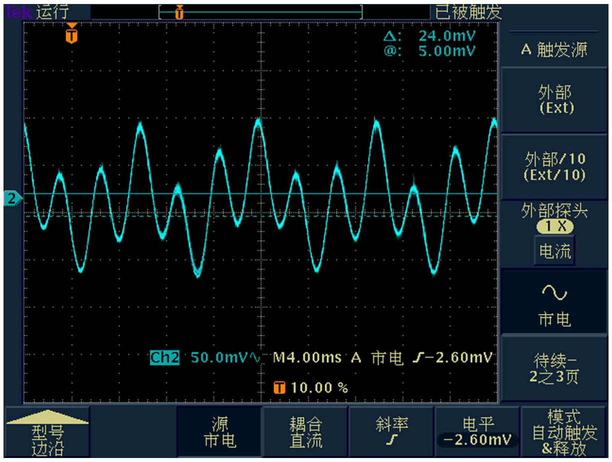

Fig. 10. (color online) Waveform of current ripple with MPS working at 24 A.

Figure 11 shows the current waveform after the APF was connected. It can be seen that the APF can effectively decrease the ripple through the load.

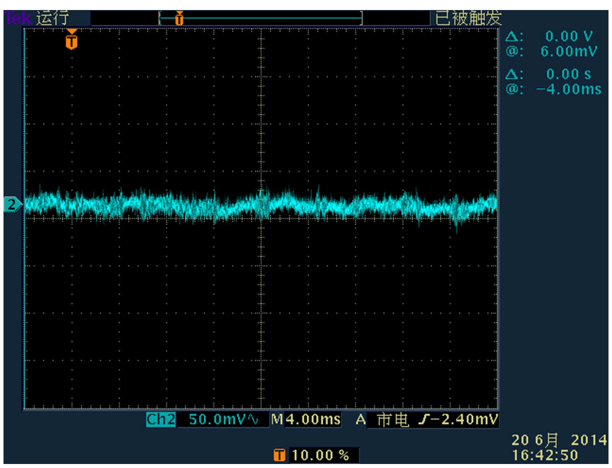

Fig. 11. (color online) Waveform of current ripple with APF connected, with MPS working at 24 A.

In Fig. 10, the amplitude of the current ripple is about 180 mV, and the APF decreases this ripple to less than 20mV. It can therefore be concluded that with this APF the current ripple is decreased to about one tenth of its unsuppressed value.

Turning the output current of the MPF to 40 A, the current waveforms before and after APF compensation are shown in Fig. 12 and Fig. 13 respectively.

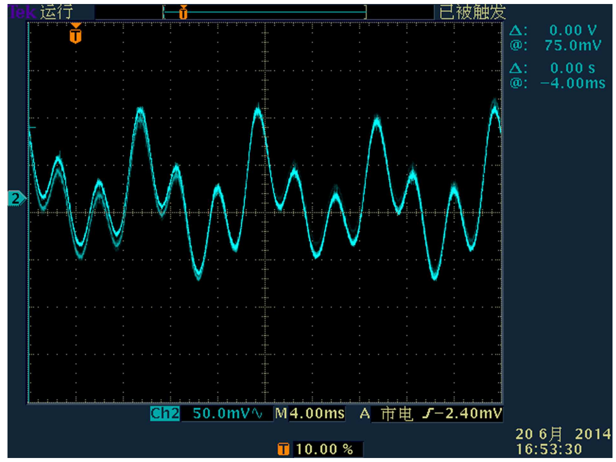

Fig. 12. (color online) Waveform of current ripple with MPS working at 40 A.

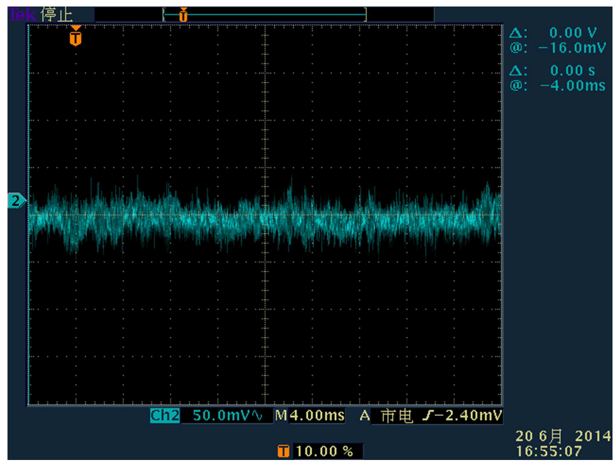

Fig. 13. (color online) Waveform of current ripple with APF connected, with MPS working at 40 A.

4 Conclusion

The following conclusions can be drawn from the experiment described above.

1) The APF in this paper can give dynamic and online compensation for the MPS current ripple. With this APF, the MPS current ripple can be reduced to a tenth of its original value.

2) The effort of the compensation effect becomes worse while the MPS current is changing, such as the current changing from 24 A to 40 A in this experiment. However, after the MPS current adjusts to a new stability, the APF can track the change, and ultimately realize the decrease of the MPS current ripple.

3) With the APF, the current ripple is obviously decreased, which enhances the accuracy and stability of the current from the MPS. However, the stability is also affected by the environmental temperature, which cannot

be improved by this APF, and thus to improve the long-term stability, a lot of research needs to be done, such as adding a temperature control-loop to the APF.

4) In the controller, the bandwidth of the APF can be verified by changing the parameters of the digital filter. To make it adaptable to most MPS systems, the bandwidth is set to 1000 Hz in this experiment. Due to the experimental conditions, compensation for high frequency ripples has not been performed.

5) This APF is totally independent of the MPS system, thus it can be installed or removed conveniently according to the MPS requirements.

6) The effect of this APF can be further improved. For this purpose, the AD samples to MPS current need much higher precision and the chosen capacitor in the APF circuit should be reconsidered. In addition, the circuit of this APF needs further research and experiments.

References

1 X. L. Guo, and J. Cheng, Chin. Phys. C, **38**(11): 86–90 (2014)
2 H. Sasaki et al, IEEE Trans.P.A.S., **90**(5): 2009–2019 (1971)
3 B. M. Bird et al, Proe. IEE, **116**(10): 1730–1734 (1969)
4 L. Tanner, Digital Control for Highest Precision Accelerator Power Supply, in *Proceedings of the 2001 Particle Accelerator Conference* (Chicago: World Scientific, 2001), p.3681